Dynamic Hydrology of a Mangrove Island: Twin Cays, Belize

Daniel W. Urish, Raymond M. Wright, Ilka C. Feller, and Wilfrid Rodriguez

ABSTRACT. The hydrology of an overwashed mangrove island is shown to be both complex and dynamic, with a strong interaction between tide-induced flow and the resident red mangrove (*Rhizophora mangle* L.) root system. A topographic map of the tidally flooded area of the island was made and related to the tide-induced water levels. The flooded area approximately doubled during the usual tidal event. The bottom topography is highly irregular with a maximum channel water depth of about 1.5 m, but much of the flooded area experiences a water depth of less than 0.5 m. Water elevations were recorded by automatic water level loggers for periods of time up to 9 months. The usual symmetrical parabolic tide signal was transformed into a highly asymmetrical form as it moved landward through the tangled root system of the red mangrove forest. A normal tide range of 13 cm at the island margin attenuated to 3 cm at a distance of 200 m landward, with a lag time of 2 h for highs and 6 h for lows. Maximum flow velocities of 5 cm/s were measured in the main channels with marked reduction in regions of dense mangrove root and shallow water depth. The combined frictional resistance of the bottom and associated mangrove roots is characterized by a Manning's roughness coefficient, n, that ranged from 0.084 to 0.445. The changing flow pattern within the flooded mangrove swamp was mapped during a 7 h high-to-low tide period using aerial photography to track the movement of slugs of visible dye placed at three locations. Analysis of the sequential time-related photos showed limited lateral dispersion in the tortuous main channel but strong tidally controlled flow direction changes and dispersion along the channel axis. A strong circulatory pattern is observed in a shallow pond at the south central terminus of the tidally affected flow system. This large shallow pond is sparsely populated by dwarf red mangrove and is some 350 m from a primary connection with the surrounding lagoon. Poor flushing of the pond creates water temperatures ranging from 25°C in the winter to 40°C in the summer. High surface water evaporation creates a hypersaline condition of 45 ppt salinity in summer. In winter, with the infusion of fresh rainwater, salinity of surface water in the pond can be less than 5 ppt. Because of its role in the transport of nutrients and detritus, and its flushing action, the dynamic hydrological system of the mangrove island is a highly important ecological feature of the overwashed mangrove island.

Daniel W. Urish, Raymond M. Wright, and Wilfrid Rodriguez, University of Rhode Island, Engineering Department, Bliss Hall, 1 Lippitt Road, Kingston, Rhode Island 02881, USA. Ilka C. Feller, Smithsonian Environmental Research Center, 647 Contees Wharf Road, Edgewater, Maryland 21037, USA. Corresponding author: D. Urish (harbourrose@cox.net). *Manuscript received 13 May 2008; accepted 20 April 2009.*

INTRODUCTION

Mangrove forests are tropical wetlands with a specialized vegetation adapted to waterlogged and saline conditions (Lugo and Snedaker, 1974; Hutchings and Saenger, 1987; Ball, 1988). These forests provide energy-absorbing buffers from

hurricane-driven seas, prevent coastal erosion, provide a protective habitat for many fish juveniles, and are a nutrient source for the surrounding waters (Odum and Heald, 1972, 1975; Twilley, 1988; Danielson et al., 2005; Barbier, 2006, Constanza et al., 2008), as well as a filtering mechanism for sediments and pollution (Alongi and McKinnon, 2005). Under natural conditions mangroves live in a highly dynamic environment and in synergistic balance with their natural neighbors. Mangroves have evolved features that enable them to cope with an ever-changing regime of tidal water ranges, variable salinity and temperature, and anoxic soil conditions, but within limits (Tomlinson, 1986). The biggest enemy appears to be man, who can directly or indirectly destroy, in days, whole mangrove communities that have taken thousands of years to develop (Alongi, 2002; Macintyre et al., 2004; Rodriguez and Feller, 2004; Taylor et al. 2007; Duke et al., 2007).

It is widely recognized that hydrological patterns determine mangrove structure and function at the ecosystem scale (Lugo and Snedaker, 1974; Forman and Godron, 1986; Twilley, 1995), and general models of mangrove hydrodynamics have been developed (Wolanski et al., 1992). In these coastal wetlands, tidal flooding and surface drainage influence many ecological processes, including habitat quality, water movement, filtration, and nutrient cycling (Forman and Gordon, 1986). Water flow also influences the dispersal and establishment of mangrove propagules (Mazda et al., 1999).

The significant role of vegetation and the effect of intertidal root density on tidal movement in mangrove channels has been described by Wolanski et al. (1980) and over the broader mangrove swamp environment by Wolanski et al. (1992), Furukawa and Wolanski (1996), Mazda et al. (1997), and Mazda et al. (2005). Thus, there is a synergistic relationship for the development and growth of a mangrove forest that depends on the dynamics and magnitude of tidal inundation into the swamp. Concurrently, the frictional resistance of the mangrove roots controls the degree of tidal inundation and patterns of movement in the mangrove swamp (Wright et al., 1991).

Based on long-term experiments on offshore mangrove islands in Belize, hydrodynamics have been linked to distinct patterns of nitrogen (N) and phosphorus (P) limitation across the intertidal flow system (Feller et al., 2003). Lovelock (2008) suggested that differences in tidal inundation also influence soil respiration and belowground carbon sequestion via root production, which is the source of the deep peat deposits underlying these islands. McKee et al. (2007) predicted that the ability of islands such as Twin Cays to keep pace with rising sea levels is dependent on the tight coupling between peat formation and hydrology.

Although these and other studies based at Twin Cays have identified tidal flooding as an important drive of ecological processes, there is limited knowledge on the specific pattern of water movement across these islands. Thus the objective of this research was to conduct a detailed analysis of tidal characteristics and flushing patterns of West Island, the smaller of the two main islands in the Twin Cays Archipelago.

Location

The Twin Cays Archipelago lies some 22 km off the coast of Belize (Figure 1) on the edge of the Belizean Barrier Reef (16°50′N, 88°06′W). Islands of the Barrier Reef and its surrounding waters have been the locations for scientific ecosystem studies by the Smithsonian Institution since 1972 (Rützler and Macintyre, 1982). Because of their pristine condition and relative isolation from anthropogenic effects, the islands and contiguous waters of Twin Cays were selected for detailed scientific research of oceanic mangroves and associated marine ecosystems (Rützler and Feller, 1996). Field studies of the dynamic hydrology of the Twin Cays mangrove ecosystems were begun in 1986 and have continued since that time. This particular study focuses on the surface hydrology of West Island of Twin Cays (Figure 1), a 21.5 ha kidney-shaped landmass approximately 900 m long and 400 m wide. According to the classification of Lugo and Snedaker (1974), the island is an "overwashed mangrove island," one frequently overwashed by tides and with high organic export.

Island Characteristics

The land cover on West Island and effect of man are shown in Figure 2, which depicts the natural mangrove growth and the man-made clear-cut and dredge-fill as mapped by I. C. Feller of the Smithsonian Institution in 2002. Since then even more mangrove destruction has occurred on the east side of the island. The island is dominated by the red mangrove, *Rhizophora mangle* L., with black mangrove (*Avecennia germinans* L.) on somewhat higher topography in the intertidal zone and white mangrove (*Laguncularia racemosea* L.) above the intertidal zone (Rützler and Feller, 1988; Rodriguez and Feller, 2004). It is to be noted that the density of the mangrove is far from uniform, with sparse dwarf red mangrove dominating the interior, and much more vigorous red mangrove growth on the island perimeter

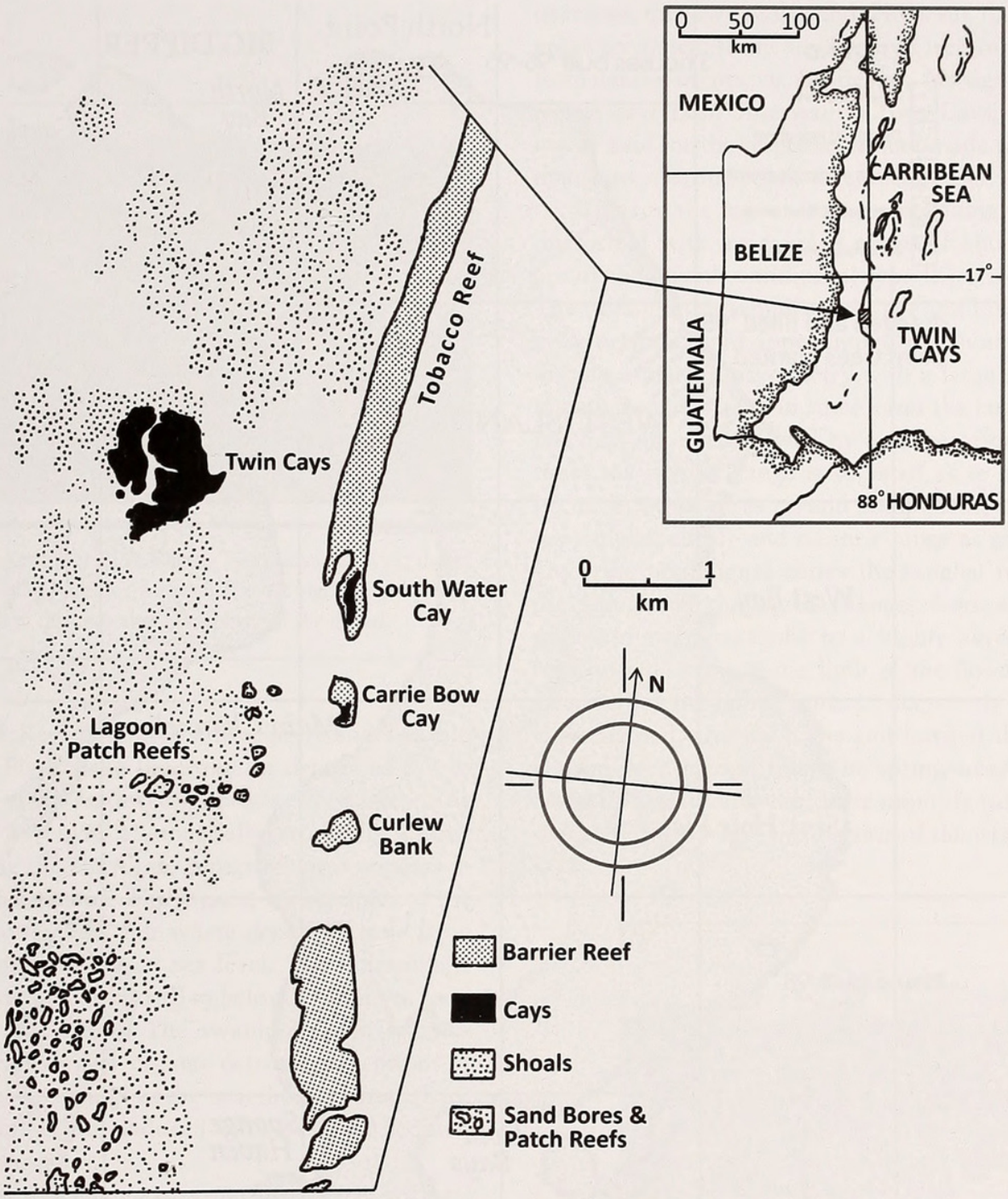

FIGURE 1. Location map of Twin Cays, Belize, Central America. (Adapted from Rützler and Macintyre, 1982.)

and in areas of greater tidal movement. Figure 3 is a photograph taken from the island interior showing the dwarf red mangrove in the foreground and the distant background of taller dense red mangrove growth that characterizes the island perimeter. Figure 4 provides a botanical rendering of the cross section of the scrub red mangrove, showing the relationship between mangrove foliage, stem and root structure, average tidal range, and hydrogeologic strata. It is to be noted that the typical low tide level is near the top of the organic ooze.

The mangroves of Twin Cays have developed on an ancient limestone plateau over the past 8,000 years (Macintyre et al., 2004). During this time 9–12 m of Holocene mangrove deposits have accumulated on the underlying limestone substrate and kept pace with rising sea level (Toscano and Macintyre, 2003; Macintyre

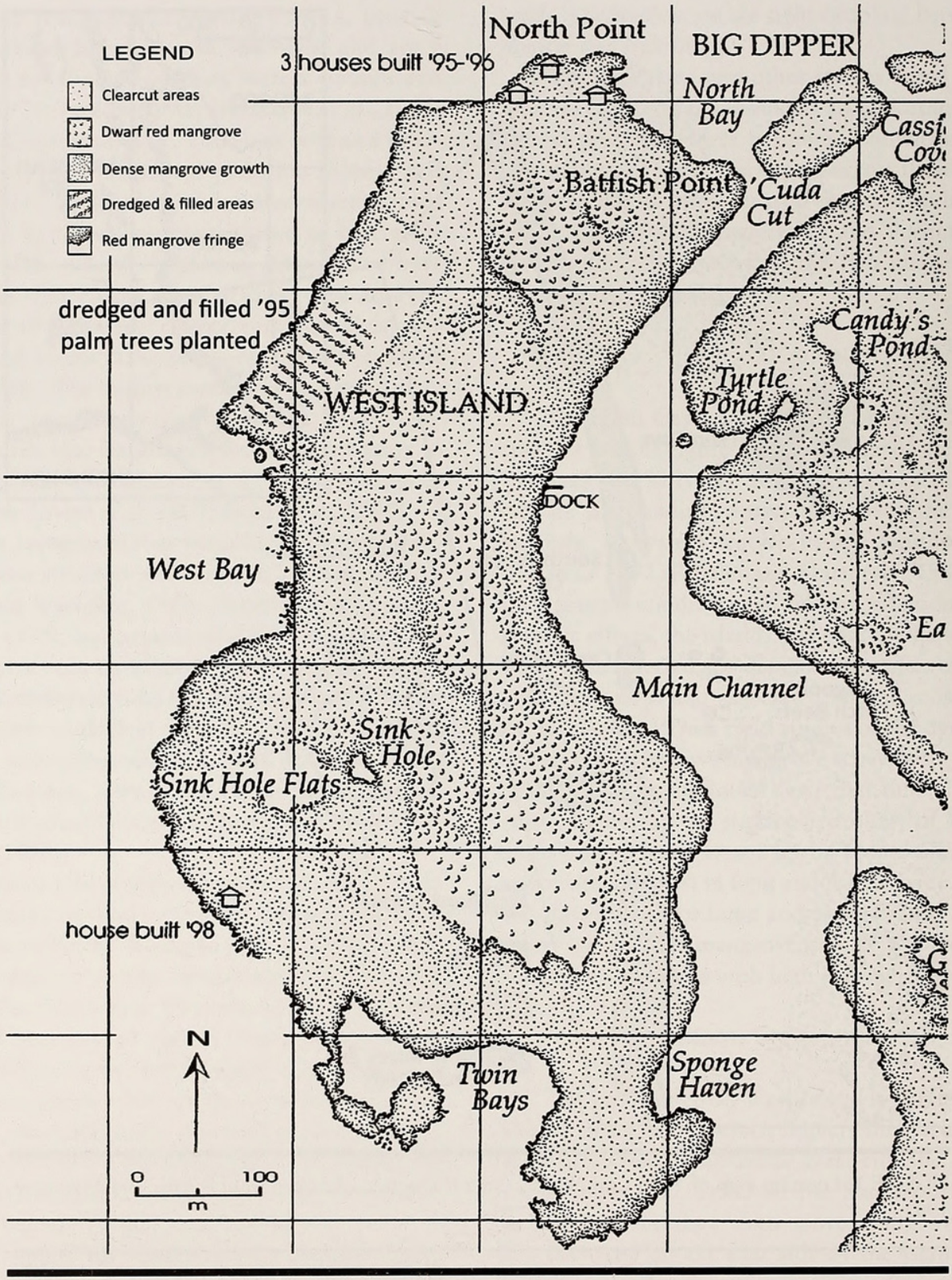

FIGURE 2. Land cover characteristics of West Island, Twin Cays, Belize, based on aerial photographs taken in 2002 that show mangrove density and clear-cut areas. (Drawn by Molly K. Ryan of the Smithsonian Institution in 2002.)

FIGURE 3. Photograph of West Island, Twin Cays, showing dwarf red mangrove of island interior with much more vigorous fringe red mangrove growth in distance along periphery of the island.

et al., 2004; McKee et al., 2007). Macintyre and Toscano (2004) found Pleistocene limestone at depths of 8.3 to 10.8 m below mean sea level in cores at West Island. As sea level rose to cover a subaerially eroded limestone plateau fringing the coastline, mangrove peat appears in the stratigraphic record. The highest topography of the island is on the seaward side where deposited sand is no more than 1 m above mean sea level. The limestone is now found at depths of 9 to 10 m below present sea level (Macintyre et al., 2004). The swamp bottom is composed largely of soft silty organic detritus. Exceptions of harder bottoms are found in the nearshore swamp channels where stronger tide-induced velocities have scoured the channel bottoms.

The climate of Twin Cays is marine tropical with air temperatures ranging during the year from 24°C in January to 29°C in June; humidity averages about 78% (Rützler and Ferraris, 1982). Lagoon water temperatures range from 23°C in the winter to 31°C in the summer. The microclimate of West Island, particularly that of the interior water, has a much greater range. The estimated annual precipitation at Twin Cays is about 1,885 mm, based on 4 years of complete records at the climatological station on Carrie Bow Cay, 4 km away. This precipitation is about 80% of the annual precipitation of the nearest mainland climatological station, the Melinda Forest Station, 30 km to the northwest. The monthly pattern is much the same for both stations. Hurricanes cause seawater to completely overwash the low-lying island. However, the natural mangrove ecosystem seems resilient and well suited to survival from natural events, viz. hurricanes. No significant adverse effects have been observed on Twin Cays; the same cannot be said for the response to man-made features, where mangrove clearing results in severe coastal erosion.

Tides in the lagoon area surrounding the island are microtidal with an average range of about 15 cm and are of the mixed semidiurnal type (Kjerfre et al., 1982). The tides exhibit semidiurnal high and lows with a tidal cycle periodicity of approximately 12 h and 25 min, but display a marked asymmetry with a large tide range following a smaller one. In some cases the larger range is as much as 40 cm, followed by a range of only 10 cm. At times the smaller range is so small as to appear nonexistent. In other cases certain components of the tide occur simultaneously and create a range as great as 50 cm. Once the tidal signal enters the tangled root system of the mangrove, the signal changes from a form that is approximately parabolic to a highly asymmetrical pattern, in which the rising limb of the flood tide is much steeper than the falling limb. Concurrently the amplitude is attenuated, and the highs and lows of the tidal signal lag the open lagoon tide. The spring–neap tidal cycle is about 29.5 days and can cause monthly tidal ranges that completely "dry up" the interior of the island.

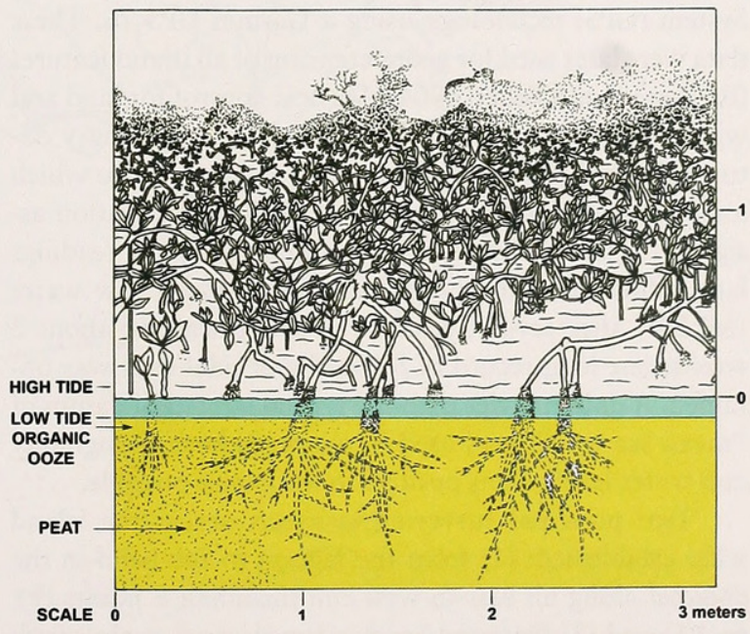

FIGURE 4. Botanical rendering of cross section of dwarf red mangrove showing relationship between mangrove foliage, stem and root structure, average tide range, and hydrogeologic strata. (Drawn by Molly K. Ryan of the Smithsonian Institution in 1989.)

METHODOLOGY

The information required for a study of the dynamic hydrology of West Cay encompassed both spatial and temporal data and a wide variety of methods. These methods included field surveying techniques for obtaining the island topography and bathymetry, automated water level recorders for water levels, automated temperature loggers, electromagnetic water current meters, conductivity meters for determination of water salinity, and aircraft for photographic recording of dye flows, among a host of lesser equipment and measuring devices that were employed over the study period of 18 years (1988–2006).

Topography

Topography was determined for the tidal flood region extending from open lagoon water at the west side of the island along the 350 m long channel and the southern interior pond (Urish et al., 2003; Wright et al., 1991). Some 36 semipermanent monitor locations were established in 1988 in the intertidal swamp to obtain water level and water quality measurements. The locations were marked with 2 cm diameter polyvinyl chloride (PVC) pipes driven into the ground in a grid pattern. Horizontal control was established by field measurement with a 35 m long tape and conventional level and transit surveying techniques (Wolf and Ghilani, 2006), later located with Global Positioning System (GPS) technology using a Garmin GPS 76. These data were later used for georeferencing of all island features (Rodriguez and Feller, 2004). Vertical control for land and water measurements was determined from a primary datum reference point on the east side of the island to which an arbitrary datum was assigned. The initial elevation assigned to this reference point was 3.05 m with all readings later adjusted to an approximate mean lower low water (MLLW) after several years of time segments of about 2 weeks; one long record of 9 months of tidal data was obtained. A datum lower than the typical terrestrial datum of "mean sea level" was used to maintain both topography and water level values positive to the extent possible.

Two principal surveying transects across the island were established: (1) from the lagoon to the bend in the channel along an east-to-west run including 6 points (F1 to A1) and (2) from the bend in the channel to the south pond along a north-to-south run of 12 more points (A1 to A12). In addition, 3 to 5 points were determined perpendicular to each transect point. These secondary points were spaced approximately 15 m apart. These established points, as located on Figure 5, were the primary location references for all subsequent data collection.

Automated pressure transducer water level loggers (In-Situ Environmental Data Logger Model SE 1000c with pressure transducer probes) were employed at five locations for short-term (1–2 weeks) measurements. These units were vented to automatically compensate for ambient atmospheric pressure. Later in the study period 12 of these locations became long-term monitoring stations with automated self-contained water level loggers (Remote Data Systems, Navassa, N. C.) that remained in place for as long as 12 months to record data at 30 min intervals with an accuracy of about 3 mm. Self-contained automated temperature loggers (Optic Stowaway by Onset Computer Corporation) were also deployed to record temperatures at 30 min intervals for as long as 9 months. In addition to the monitor locations, stilling wells consisting of slotted 15 cm diameter PVC pipe for both manual and instrumented tide measurements were established at both shorelines of the island, and later in the study these were correlated with a primary oceanographic/climatological data collection station established at the Smithsonian Research Station on Carrie Bow Cay, 4 km southeast. The tops of the stilling wells were initially assigned an elevation based on the same arbitrary datum as used at the key datum reference points. Elevations were established on the tops of all reference station pipes using survey leveling techniques with a Topcon Automatic Level (model ATF–1A). The coordination of tides at West Island and Carrie Bow Cay was accomplished by comparison of a series of six separate short-term tidal cycle measurements taken concurrently at both stations.

Hydrology

Water flow direction and velocities during various positions of the tide cycle were determined using conventional stream gauging techniques along channel cross-sections, or "reaches:" section A–A′ was defined between survey points A1 and D1 and reach B between survey points D1 and E1. The measurements were taken at various times during the tidal cycle using a Marsh-McBirney electromagnetic current velocity meter and standard stream channel cross-sectioning methods (Watson and Burnett, 1995). Velocities and water depths were measured at 0.6- to 1.5 m intervals perpendicular to the flow to provide 25 to 50 individual measurements at each cross section. These measurements were then plotted to determine flow volumes and flow friction factors and to examine trends.

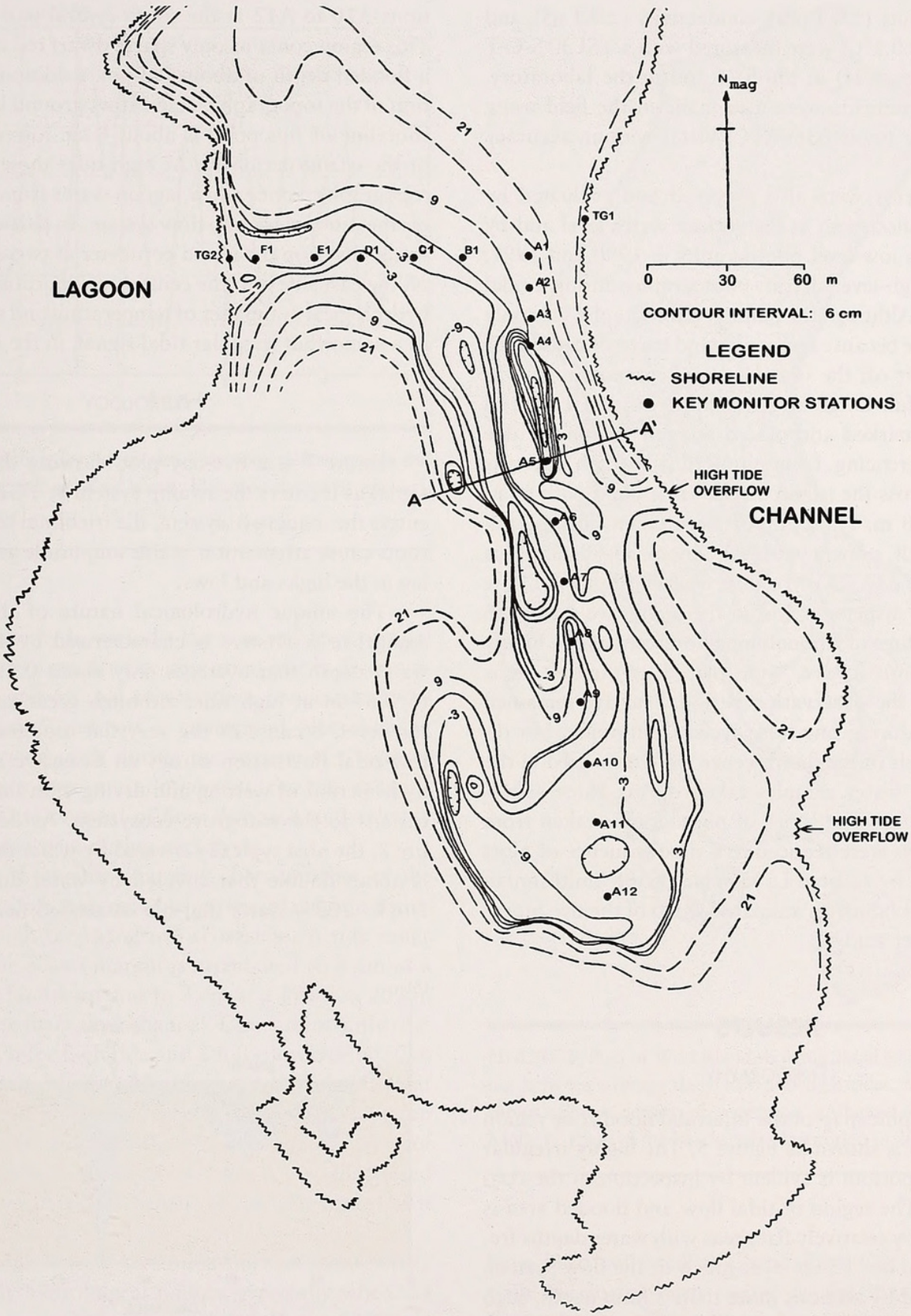

FIGURE 5. Topographic contour map of interior of West Island showing locations of key monitoring stations and representative channel cross section A–A′. Elevation datum = mean lower low water (MLLW). Contour interval = 6 cm.

Water salinity (±0.1 ppt), conductivity (±0.1 uS), and temperature (±0.1°C) were measured with a YSI 30 S-C-T (Yellow Springs, OH) in the field and in the laboratory. Salinity measurements were also made in the field using a refractometer (model 366ATC; Vista) with an accuracy of ±1 ppt.

Flow patterns were also observed and evaluated by use of dye studies, both at the surface water level and by helium balloon low-level photography in 1990 and 1991, and later by high-level aircraft photography during a tidal cycle in 1993. Although the balloon photography was only of limited value because upper air wind currents caused the balloon to drift off the island, aircraft photography was highly successful. Large targets, approximately 1 × 2 m in size, were marked and placed at each station for dye movement referencing. Continuing runs at 0.5 h intervals were made across the island on the same flight path at an altitude of 150 m. Photographs were taken during each run with a SLR camera with AF Zoom 35-70 mm lens (Minolta 5000 MAXXUM), thus enabling both the flow directions and dispersion within the mangrove system to be observed. Slugs of Rhodamine fluorescent dye, a highly visible but nontoxic dye, were placed at three stations at the start of the observation period. The dye remained highly visible during one tidal cycle. Continuing, but diminishing, levels of the fluorescence were measured in the laboratory on water samples taken during three subsequent tidal cycles. The series of photographs taken from the aircraft runs were reduced to a time sequence of plots and then used by George L. Venable of the Smithsonian Institution to produce an animated video of the dye movement for further study.

RESULTS

Topography

A topographic map of the intertidal flood zone region of West Island is shown as Figure 5. The highly irregular nature of the bottom is evident by inspection of the contour pattern. The region of tidal flow and flooded area is characterized by relatively flat areas with water depths frequently only about 25 cm over much of the flow system, but highlighted by sections more than 1 m in depth, such as occur between stations A4 and A5. Such deep holes are not necessarily coherent with the main flow channel. A cross-section (A–A′) plot (Figure 6) at station A5 depicts the extreme changes in channel bottom that exist at this location. In contrast, the other significant feature of the system is a very large shallow pond of about 2.2 ha at stations A10 to A12 at the south central part of the island. This region contains only sparse dwarf red mangrove with a flooded depth of about 0.25 m. Additionally, examination of the topographic map shows ground level at the east shoreline of this pond is about 6 cm lower than the rest of the island periphery. At high tides these limited lower topographic zones allow lagoon water from outside to enter the internal swamp flow system. In particular, high tide waters overtop the island perimeter at two other locations on the east side into the central region, causing short-term hydrological anomalies of temperature and salinity, as well as a somewhat irregular tidal signal, in the system.

Hydrology

Figure 7 is a five-day plot showing the typical tidal signal as it enters the swamp system at TG2. As the signal enters the mangrove system, the frictional resistance of the roots cause attenuation in tide amplitude as well as a time lag in the highs and lows.

The unique hydrological nature of the flow in the mangrove ecosystem is characterized by a very shallow water depth that averages only about 0.5 m at low tide to 0.67 m at high tide, although great variations exist. However, because of the very flat topography, even this low tidal fluctuation causes an extensive and significant hydroperiod of wetting and drying with important implications to the mangrove ecosystem. As depicted on Figure 8, the area typically covered by water during high tide is about double that covered by water during low tide. Doyle (2003) states that his controlled field experiments

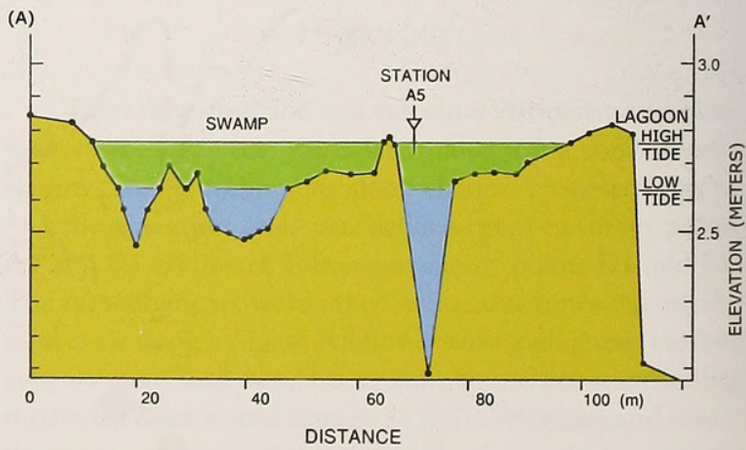

FIGURE 6. West Island cross section A–A′ at station A5 showing relative relationship of high and low tides to bottom contours. Green = range of flooding from the tide; blue = low tide flow. Elevation datum is arbitrary.

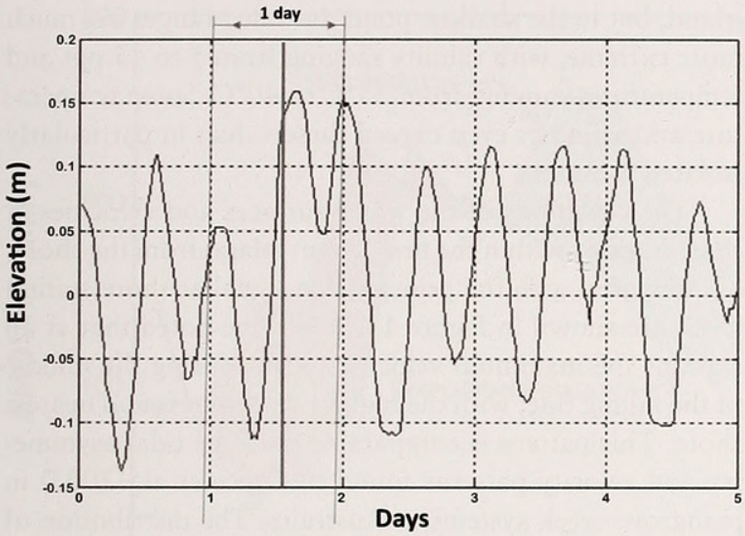

FIGURE 7. Plot of five-day tide sequence showing relative ranges and asymmetry of the tide at West Island. Elevation datum = approximate mean sea level.

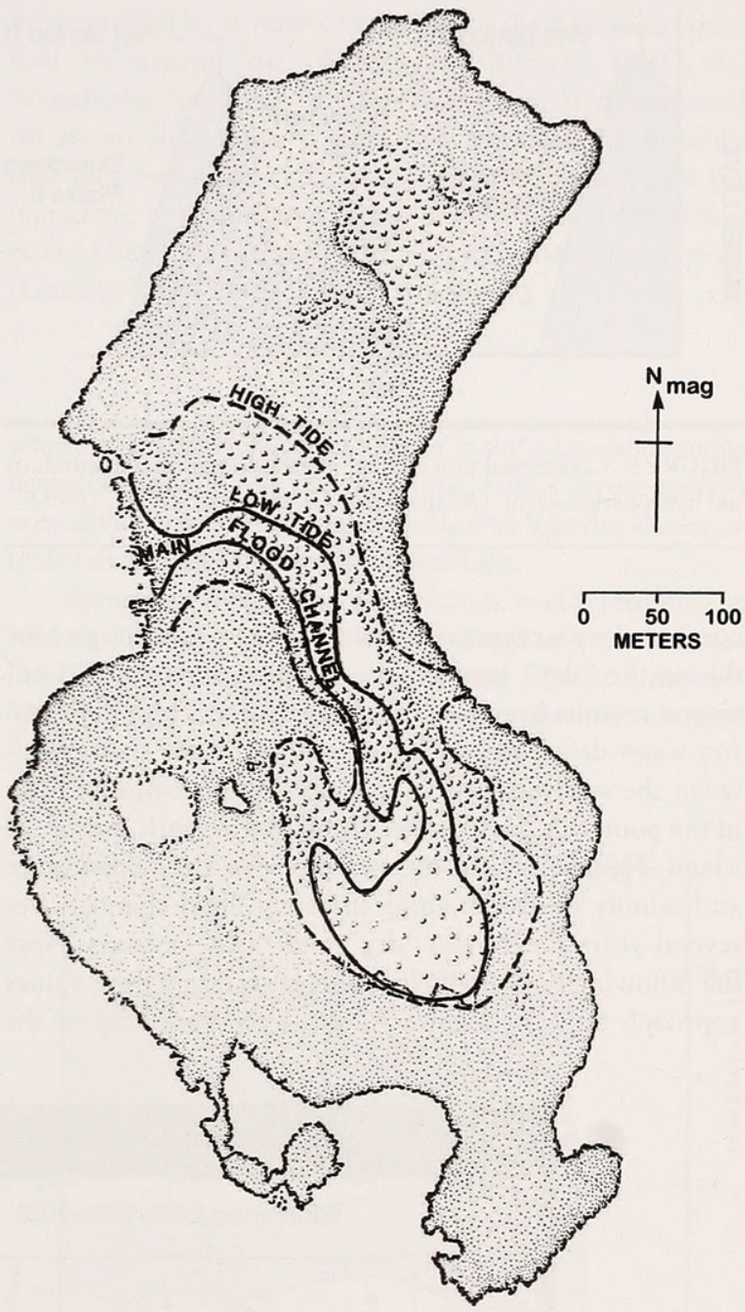

FIGURE 8. Plan of West Island showing aerial extent of tidal flooding between average daily low and high tides. Stippling on map shows relative density of vegetation. (Adapted from drawing by Molly K. Ryan of the Smithsonian Institution in 2002.)

"suggest that the hydroperiod—the rate and level of tidal exchange—plays a much more important role in determining mangrove growth and success than previously documented." Figure 9 presents a conceptual plot showing the wetting–drying cycle during the sequential phases of the tide. Perhaps even more important, the tide range is sufficient to cause reversal of flow direction and velocity throughout the system during each cycle.

Figure 10 shows the changing characteristics of the tidal signal at three stations as it moves inland in a tortuous path through the mangrove ecosystem. A tide range of 13 cm at the island margin is attenuated to 8 cm at a location 50 m landward and to 3 cm at a location 200 m landward in the main flow channel. Concurrently, there is a lag time of 1 h for high tide and 2 h for low tide at 50 m landward, and of 2 h for high tide and 6 h for low tide at 200 m landward. The great difference in lag time between highs and lows is caused by the much greater influence of root density during a receding tide; this is also illustrated by the asymmetrical characteristic of the tidal signal as it transposes landward.

The seasonal climatic variations had a profound effect on the monthly hydrological budget, especially when the high evapotranspiration was considered. Figure 11 shows the approximate seasonal relationships of precipitation, surface water evaporation, and vegetation transpiration (evapotranspiration), assuming a total annual rainfall of 1,885 mm. This value and the estimated monthly values are based on limited (about 5 years) available data that have been collected at Carrie Bow Cay and correlated with the longer-term record at the mainland Melinda Forest Station. The potential evapotranspiration values for each month were calculated from the Thornthwaite equation (Dunne and Leopold, 1978; Thornwaithe and Mather, 1987) using a partial record of temperature and solar radiation available for Carrie Bow Cay. Examination of the water budget shows a deficit of precipitation as

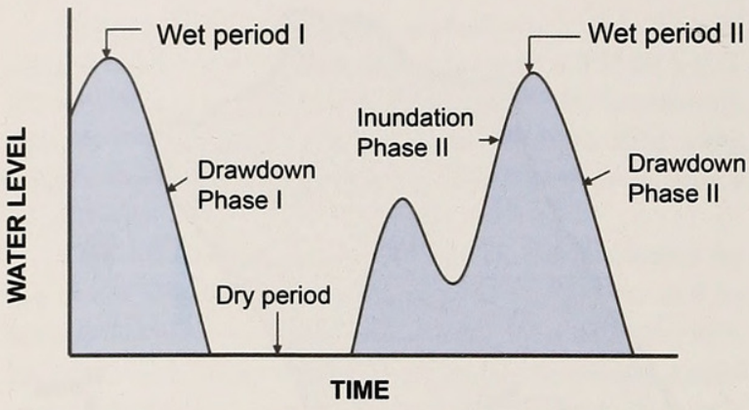

FIGURE 9. Conceptual plot of tidal phases during mixed semidiurnal hydroperiod event. (Adapted from Boulton and Brock, 1999.)

compared with evapotranspiration February through June during the "dry" season and a surplus during the "wet" season months from July through January. This "dry" season water deficit has an extreme effect on the surface water in the semienclosed interior swamp system, especially in the poorly flushed shallow pond at the south end of the island. Figure 12 is a composite plot of water temperature and salinity measured along the main flood channel over several years during the "dry" and "wet" seasons. Near the inflowing/outflowing location at station F1 the values approach those of lagoon water at the periphery of the island, but in the shallow pond the value ranges are much more extreme, with salinity ranging from 5 to 45 ppt and temperatures ranging from 25°C to 40°C. Some temperature and salinities even exceed these values in particularly isolated locations.

The elevations of the water surfaces and velocities at three stations within the first 150 m inland from the shore, as compared with the primary tide signal at shore station TG2, are shown in Figure 13. It is to be noted that at all stations the maximum velocities occur during the middle of the falling tide, with the highest velocities found nearest shore. This pattern is comparable with the tidal asymmetry and velocity patterns found by Bryce et al. (2003) in mangrove creek systems in Australia. The distribution of flow and variations of velocity for a typical channel section are illustrated in Figure 14 for a cross section at station A4. The data were acquired during a mid-tide flood tide at a time of maximum velocity. The upper part of Figure 14 shows depths of water across the section at the specific time of the velocity measurements shown in the lower part. The velocities shown are an average determined from a series of velocities measured at a series of depths over the shortest time period possible. As indicated the velocity changes dramatically, from 2.0 to 0 cm/s, across the section, although there is a general pattern of greater velocity at the deeper parts. However, this is contradictory to the observation that the deeper part on the right side does not

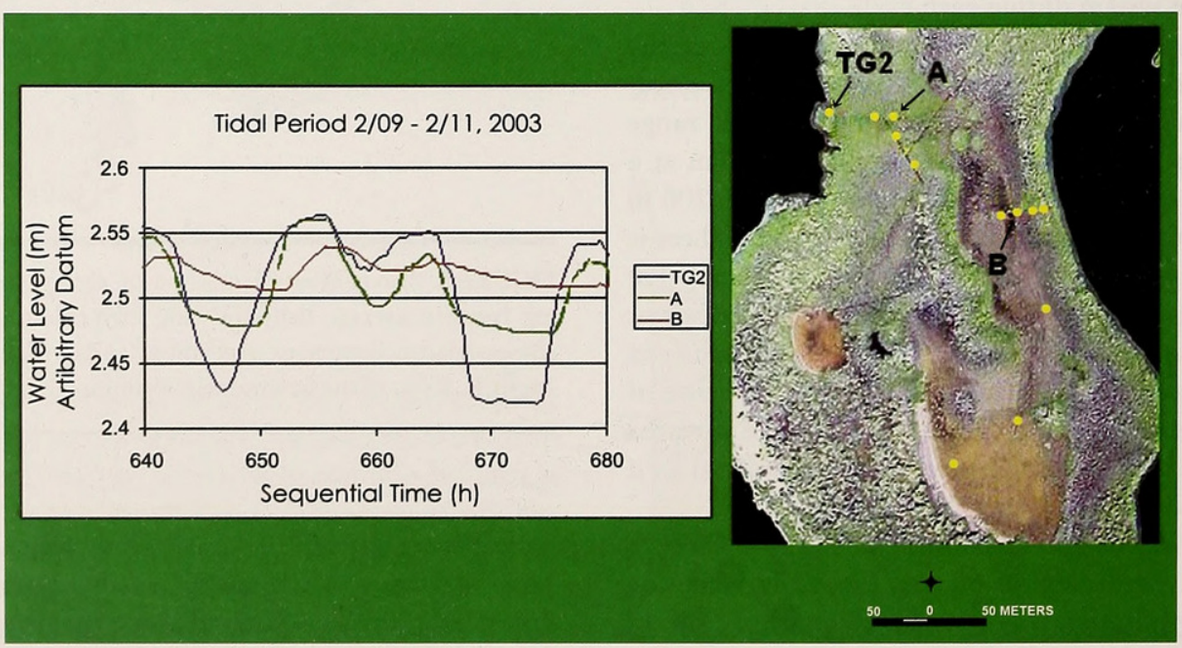

FIGURE 10. Tidal fluctuation plots at three interior monitoring stations—TG2, A, and B, as shown on photograph at right—during maximum velocity of flood tide on 27 May 1988. Yellow dots on the photograph are locations of monitor stations. Elevation datum is arbitrary.

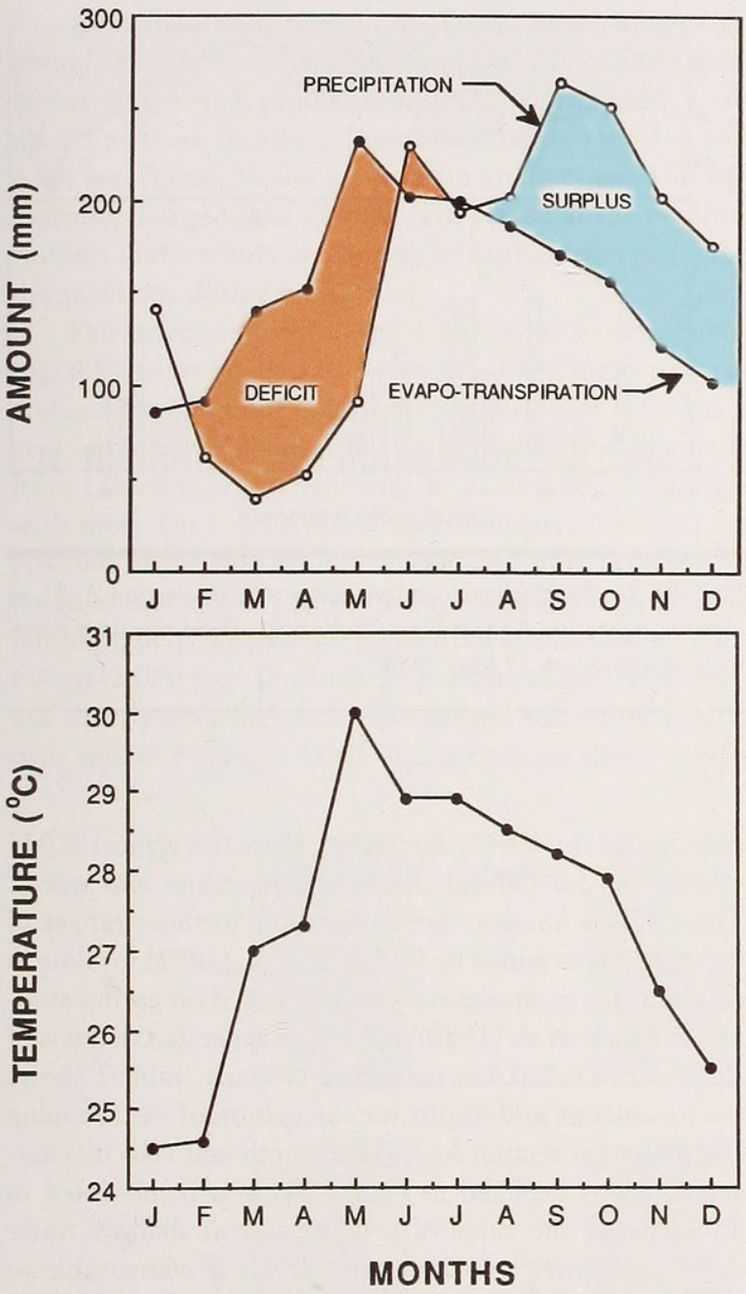

FIGURE 11. Hydrological budget for West Island showing annual pattern of precipitation, evapotranspiration, and temperature. Shaded orange area = the "dry season" with net deficit of water from evapotranspiration; blue shaded area = the "wet season" with a surplus of precipitation.

have a high velocity. Inspection of the topographic plan (see Figure 5) provides the explanation: The deeper right-hand feature is a part of a closed depression, whereas the deeper part on the left is continuous with the main channel flow.

The average flow velocity between points in the swamp is reflective of both the tortuous path of flow through the mangroves and the frictional resistance of the mangrove root system and the channel bottom. This resistance can be quantified by inverse calculation of the Manning equation for stream flow (Watson and Burnett, 1995). Although the Manning equation was originally developed for stream flow, it has a logical deterministic relationship that has been used successfully by other researchers for mangrove flow characterization and modeling (Wolanski et al., 1980). The Manning equation in MKS unit format (Lindsley and Franzini, 1979) is

$$V = 1/n\, R^{2/3}\, S^{1/2},$$

where V is the average velocity, n is the Manning roughness coefficient, R is the hydraulic radius (cross-section area divided by wetted perimeter), and S is the slope, or hydraulic gradient, of the water surface.

Manning's roughness coefficient, n, was determined at various locations in the flow system and at various times in highly fluctuating stream depth and current direction. The determined values of n for these measurements ranged

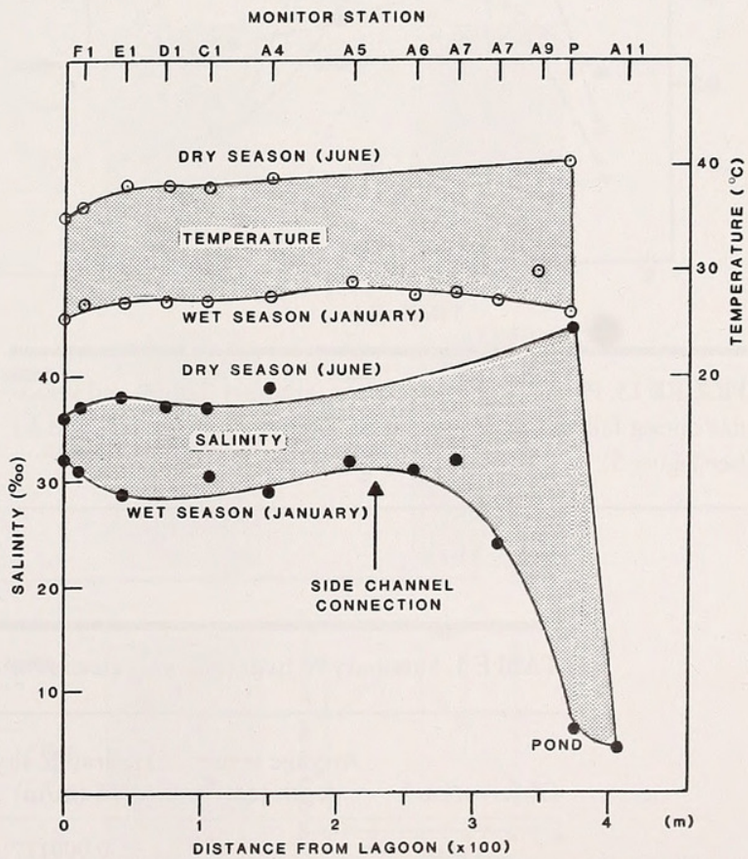

FIGURE 12. Plot showing ranges of salinity (black dots) and temperature (circles) during "dry" and "wet" season conditions at the southern shallow pond on West Island. Monitoring stations (see Figure 5) with distances from the open water lagoon at the west periphery of the island are indicated.

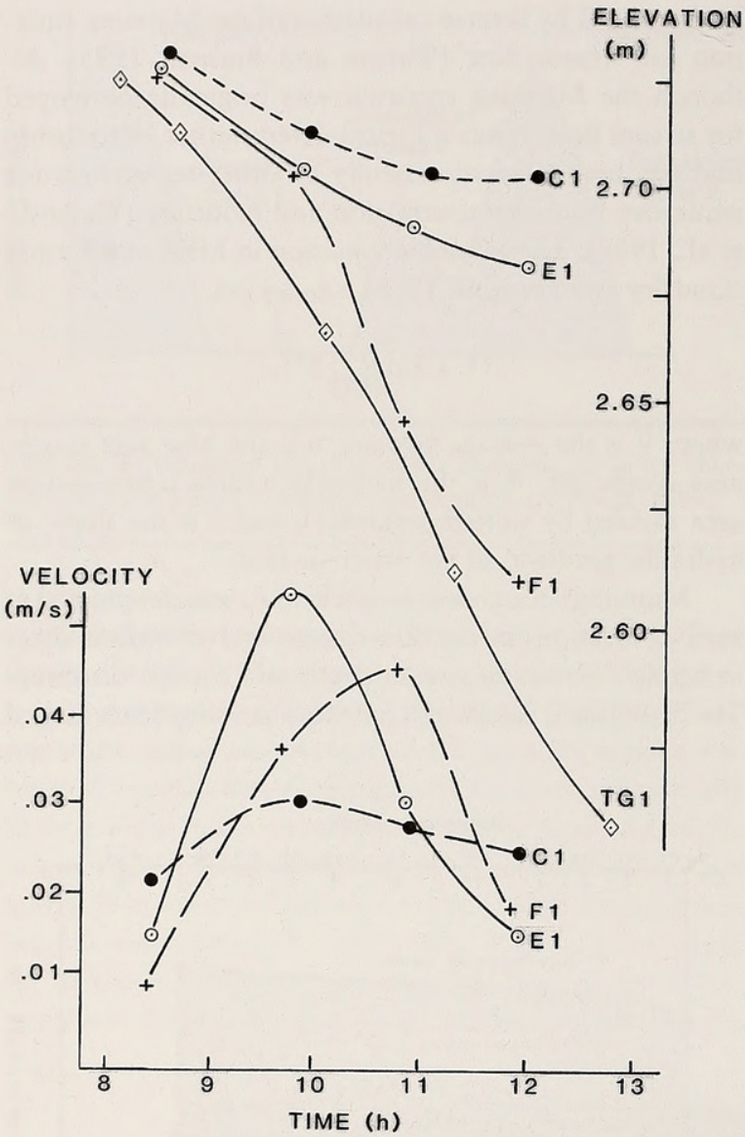

FIGURE 13. Plot of relative elevations (arbitrary datum) and velocities during falling limb of tide at monitor stations C1, E1, and F1 (see Figure 5).

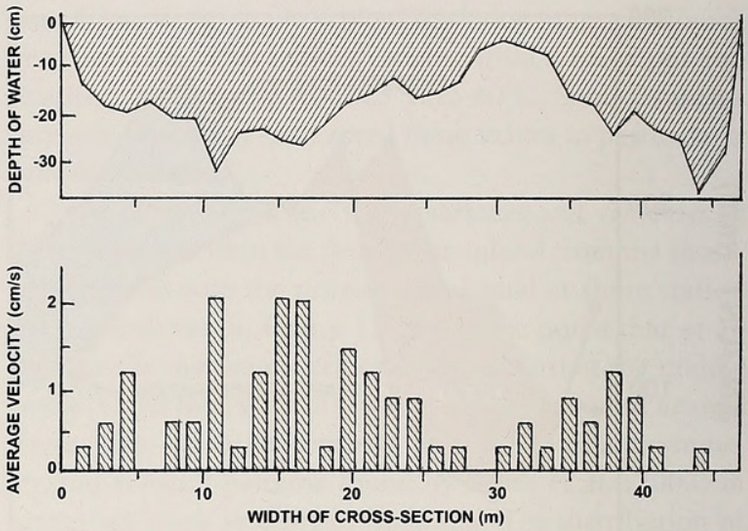

FIGURE 14. Water depths and velocities at cross-section A–A′, at monitoring station A4 (see Figure 5) during a flood tide with maximum velocities, on 27 May 1988.

from 0.084 to 0.445, far higher than the typical 0.035 found even for natural channels with stones and weeds. These values however are comparable to those ranges of 0.2 to 0.7 determined by Wolanski et al. (1992) for flow in southern Japan mangrove systems. Based on earlier studies, Wolanski et al. (1980) had earlier suggested that n is of the order of 0.2–0.4 in mangrove swamps. Table 1 shows the parameters and results for calculation of the Manning coefficient for section A–A′, with depth and velocity characteristics as depicted in Figure 14. It is to be noted in Table 1 that the value of n is greatest at shallow water depth and lower velocities. Again, this is comparable to the findings of Wolanski et al. (1992).

TABLE 1. Summary of hydraulic parameters for cross-section A–A′ at Station A4 (see Figure 5).

Observation [a]	Average water depth (cm)	Hydraulic slope, S (m/m)	Average velocity (cm/s)	Flow (m^3/s)	Manning's coefficient, n
1	11.9	0.000117	0.6	0.034	0.415
2	13.4	0.000110	0.6	0.037	0.445
3	14.3	0.000102	1.3	0.085	0.206
4	14.6	0.000098	1.1	0.069	0.261
5	16.4	0.000086	1.3	0.097	0.210
6	20.3	0.000055	1.6	0.145	0.159

[a] Each observation with the associated calculations is based on 30 measurements across cross-section A–A′ as detailed in Figure 14.

A dye flow study was accomplished during a high tide period on 5 June 1993. Single slugs of Rhodamine fluorescent dye, which produced a distinctive red color, were placed at three locations (monitor stations D1, A6, and A10; see Figure 5) along the main channel early in the morning. Large visual targets were placed at the monitor stations in the mangrove swamp to enable referencing the dye positions during movement.

The movement of dye was documented by aerial photography from an aircraft flown in a fixed flight pattern, and at a fixed altitude of 150 m (500 ft.), Runs were made at 0.5 h intervals. Figure 15 is a series of drawings made from 11 of these runs, depicting the leading edge of the dye with time. The 7 h period of measurement relative to the position of the tide at the exterior lagoon is depicted on the inset tide plot of Figure 15. Figure 16 is a high oblique photograph of West Island taken from an altitude of about 600 m (2,000 feet) showing the position of the dye at 9:10 AM, shortly after high tide. The aircraft run pattern starts over monitor station TG 2 and progresses east, turning south to proceed over the large pond at the south end of the island. The series of photographs have been converted to an animated visual program by George L. Venable of the Smithsonian Institution (URL http://www.uri.edu/cve/dye.mov) that clearly shows the oscillation of the water of the mangrove swamp water as the dye at station D1, some 70 m from the lagoon, first went to the east, then reversed to finally discharge into the lagoon. The dye flow at station A6 also oscillated, then merged with the outgoing dye from station A10 approximately 120 m south of A6, toward the pond. Interestingly, the dye placed at A10, at the north margin of the pond, also moved into the pond and then flowed in a circulatory pattern. This pattern may be caused by new lagoon water overflowing the rim of the pond to the east because the tide during the period of observation was a relatively high spring tide. Finally the dye from D1 discharges into the lagoon, and the merged A6/A10 dye moves north. Previous water level studies with measured levels of fluorescent dye indicated that this dye persists at continuing reduced levels in the central locations

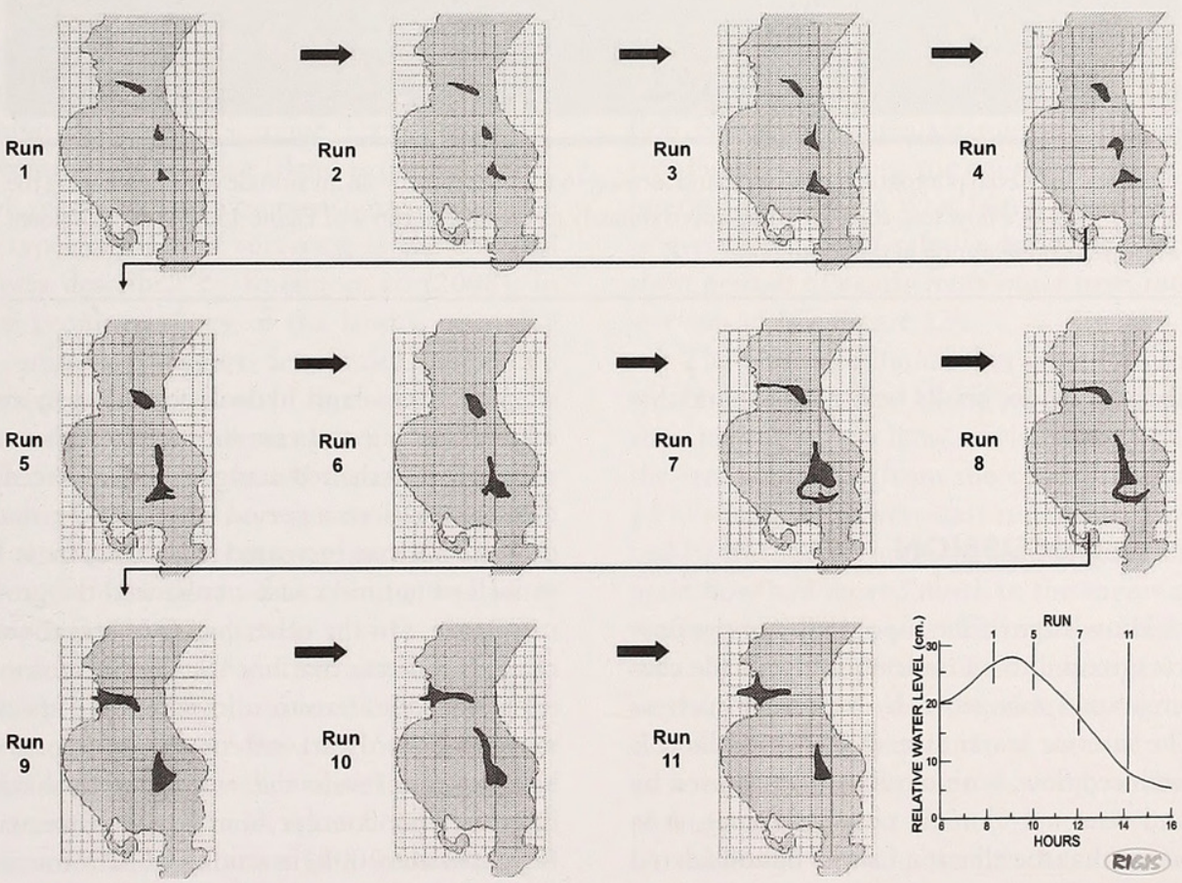

FIGURE 15. Sequential plots of dye flow patterns over a 7 h period from high tide through low tide, during dye flow test on 5 June 1993. The plot in the lower right-hand corner shows the relative time position of runs with tide levels at station TG2.

FIGURE 16. Aerial photograph of West Island looking to the northwest from an altitude of 600 m during the 5 June 1993 dye flow test, corresponding approximately to the time of run 4 of Figure 15. The dye is evident as the red configuration in the south pond.

for several tidal cycles before finally being flushed and dissipated into the lagoon.

DISCUSSION

An intimate knowledge of the topography of the flow and flood area is essential to an understanding of the ecosystem of a semiclosed mangrove hydrosystem such as West Island. The interior water system of West Island is primarily tide-induced flow, with modifications caused by precipitation and seasonal climatic change. Hence, it is also very important that the climatic factors be considered in conjunction with the hydrographic characteristics.

The tidally induced hydrodynamics of the water flow in tidal channels and ponds of an overwashed mangrove island, in conjunction with the topography, greatly affect the ecosystem and vitality of the resident mangrove systems. Analysis of the temporal and spatial characteristics of a 21.5 ha island hydrological flow system shows that where flooding and current flow becomes more vigorous, the growth of the red mangrove is enhanced. It was found, during the 18-year period of this study, that hydrological changes such as increased tidal flow, from anthropogenic as well as natural causes, enhanced the growth of the red mangrove. On the other hand, observations of relict tree remains indicate that historically the interior of the island experienced a transition in mangrove species from black mangrove to dwarf red mangrove, possibly because of higher water levels and with poor flushing in the island interior. This concept is in concurrence with findings of Knight et al. (2008) in studies of patterns of tidal flooding within a mangrove forest in Southeast Queensland, Australia, that "mangrove basin types represent a succession in mangrove forest development that corresponds with increasing water depth and tree maturation over time."

Detailed mapping of the topography of the intertidal interior region of the island reveals poorly defined flow

channels that vary greatly in depth and width. Within this system anomalous deep sections exist, further contributing to the complexity of flow. The root structure of the mangroves and the irregular bottom result in a frictional resistance to the flow, quantified by Manning's n as being as much as 10 times greater than that of conventional terrestrial stream channels. In studies in mangrove swamps on Iriomote Island, Japan, Kobashi and Mazda (2005) stress the importance of the hydraulic resistance of mangrove vegetation in determining the flow patterns, especially in reducing the velocity component perpendicular to the main channel. Accordingly, the interaction of the mangrove itself is a determinate factor in stream flow and the resulting flushing action, important to the vitality of the mangrove. It appears to be particularly relevant to the transport of nutrients and other physicochemical conditions important to the growth of the mangrove. The driving force for the flow within the mangrove hydrosystem is the ever-changing hydraulic gradient induced by the tide. Accordingly, the flow moves, at varying velocities, in and out of the interior mangrove swamp with the tide. As a result the seawater entering the mangroves not only follows a constantly changing path, but is regularly reversed in direction, and consequently it takes at least several tidal cycles for flushing of the island interior. There are indications that the central part of West Island is flooding more over a span of years, causing commensurate changes in the mangrove types capable of surviving in the changed regime, a process described by Knight et al. (2008). In other areas the geomorphology of the land is changing consequent to sediment transport, detrius deposition, and subsidence from peat compaction. In this regard Bryce et al. (2003), in studies of a small mangrove creek system near Townsville, Australia, evaluated the role of hydrodynamics in the sediment transport process. Importantly they observed that sediment transport appears to be a seasonal phenomenon, with net flux going either landward or seaward, but they conclude that the net sediment transport for the overall system may be close to long-term equilibrium. They do state that mangrove swamp areas (in the tidal overflow regions) are most likely to be places of sediment accumulation; if so, the more shallow areas of West Island, when flooded at high tide, may experience accumulation from redistribution of sediment within the system as well as from direct leaf drop and in situ detritus accumulation.

The data showed that the annual pattern of precipitation and temperature greatly affects temperature and salinity in the poorly flushed interior pond. On an annual basis there was a net discharge of water from island to the exterior lagoon because of precipitation. However, when the monthly climatic factors are considered it is apparent that during the "dry period" of February to May there is a net loss of freshwater in the island water budget, with high evaporation creating high-temperature hypersaline water in the interior. When the island is in the rainy season, July through December, the reverse is true, with the interior water becoming cooler and fresher from the rains (see Figure 12). In the extreme case, as described by Wolanski et al. (1992) for tropical mangrove systems on the coast of northern Australia, "The balance between rainfall and evaporation, in conjunction with tidal variations, is the key factor in determining if the upper levels of the swamp are (tidally flushed) swamp or (hypersaline) tidal flat." A further important implication for the shallow pond in the south part of West Island is, as stated by Wolanski et al. (1992), "rainfall significantly affects porewater salinity and it is likely that it also affects nutrient levels within the swamp substrate, particularly in areas where regular flooding by the tides does not occur." On West Island, during the "dry period" of February through May, evapotranspiration is approximately three times that of precipitation. However, during the "wet period" of June through December, conditions are reversed with evapotranspiration being approximately one-half that of precipitation (see Figure 11). Thus, the net effect on the poorly flushed interior areas of the West Island mangrove system is that of greatly increased salinity during the "dry season" and short periods of nearly fresh water from rain storms in the wet season (see Figure 12).

The effects of human intrusion into the natural ecosystem are illustrated by Figure 17, an aerial photograph showing the survey lines newly cut in 1993. At that time the strongest flow from the coastal seawater was some 25 m south of the west–east running survey cut, as identified by the darker, more vigorous vegetation. By 2003 the main flow had moved north to the survey cut itself as the cutting as well as foot traffic in the cut had deepened that area. During the course of the investigations, it was observed that the previous dwarf red mangrove trees alongside these survey lines initiated signs of vigorous growth as a result of the increased flushing, as illustrated by the photograph in Figure 18.

Although previous studies have shown that for the past 8,000 years the mangrove growth has managed to keep up with rising sea level because of peat accretion, the future may be in doubt because of anticipated greatly increasing sea-level rise rates (Mckee et al., 2007). The ability of the island to adjust to rising sea level has important implications for a future that will include sea levels rising

FIGURE 17. Aerial photograph taken in 1993 (looking south) showing survey lines that were newly cut in 1993. The original principal tidal flow path is evident as the darker green vegetation approximately 30 m south of the 1993 east–west survey line.

at a rate much greater than that experienced over the past 8,000 years when mangroves first appeared and flourished on Twin Cays. As McKee et al. (2007) have stated, "Rates of subsurface plus subsurface (root) accretion in fringe, transition and interior zones at Twin Cay were 10.4, 6.3, and 2.0 mm/year. Fringe mangroves have kept up and could accommodate eustatic sea level rise of 4 mm/year if current rates of accretion were maintained. If eustatic rates exceed 5 mm/year then these mangrove islands would not be likely to persist, assuming all other conditions remain unchanged."

The islands of Twin Cays, with a history of comprehensive ecological research, remain an important location for measuring and evaluating changes in the mangrove and associated ecosystems because they occur in a world of dramatic coastal change. Much analytical work remains to link the dynamic hydrology of the mangrove island to the physiological parameters essential to mangrove growth. The research site of Twin Cays, with three decades of baseline data and research, is a very important asset for better understanding the ecosystem of the mangrove. It is very important that this work continue and build on the substantial foundation of information that now exists.

CONCLUSIONS

Overwashed mangrove islands are extremely complex ecosystems. They are essentially self-dependent, and the vitality of the resident mangrove species is primarily a result of the tide that produces the essential hydrological functions of flushing and nutrient transport. The topography, the geomorphology, and even the existence of a mangrove island are products of the island vegetation itself. This interaction affecting the island configuration is constantly changing as the mangrove forest with its multiple species adjusts to higher sea levels and the resultant changes in hydrological flow and flooding parameters.

The interior of the island is subject to extremes of temperature (20°–40°C) and salinity (5–45 ppt) with limited flushing that may adversely affect the vitality and existence of the mangrove, as well as the natural selection of mangrove species. A comparison of the hydrological parameters and flow regimes in the regions of vigorously growing red mangrove with that of dwarf red mangrove strongly suggests that enhanced communication with external lagoon water is best for the vitality of the red mangrove on Twin Cays.

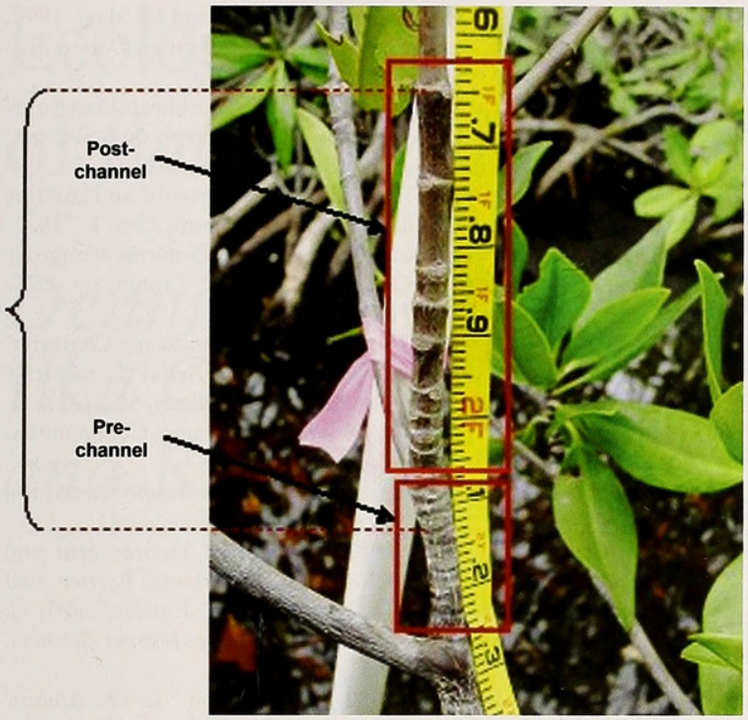

FIGURE 18. Photograph of red mangrove branch taken in 2003 near monitoring station D1 (see Figure 5) showing progressive increase of growth between sequential growth rings after survey lines were cut approximately 10 years previously. Note that the tape is marked decimally in feet.

The flow within the island is strongly influenced by the substantial frictional resistance of the mangrove root system. This dense root system serves to greatly attenuate the tidal amplitude as it progresses into the island, creating a reduced hydraulic gradient for water movement. The resultant reduced flow creates a poorly flushed island interior with poor mangrove growth.

Extensive land clearing, especially along the coastal margins, has long-term continuing effects of mangrove loss from which the island may never recover (Macintyre et al., 2009). In contrast, limited incursions such as the observed survey line cutting may shift, but enhance, channel flow, promoting more vigorous red mangrove growth. In extensive field research (Feller et al., 2003), it was found that the patterns of nutrient availability within and among mangrove ecosystems are complex. Feller et al. (1999) showed the dramatic effects of nutrient enrichment on mangrove growth as well the changes in nutrient limitations that can take place within relatively short distances in swamp ecosystems. At least in the case of the nutrient-poor (P-limitation) condition of the sparse red mangrove in the interior of the island, the cause of nutrient limitation seems to be poor flushing, which limits the refreshing of the system with phosphorus-rich lagoon water from tidal flooding.

A further concern is that of the effect of rising sea level on the ability of the mangrove to survive. The hydrodynamics of the mangrove system greatly influences the mangrove ecosystem both by transport of nutrients and sediment and by the direct ability of the geomorphology of the island to develop to keep pace with rising sea level as it has in the past (McKee et al., 2007). At the least it appears that differential growth of mangroves will occur as flooding occurs and the hydrodynamics of the system changes.

ACKNOWLEDGMENTS

The authors are grateful to the Smithsonian Institution for the opportunity and research support provided over the past twenty years, to the University of Rhode Island for its provision of faculty and staff, especially equipment engineer Brian Gray, in conducting this research, and to the many fellow island researchers who have enriched our professional lives as a part of a multidisciplinary team. We especially thank Klaus Ruetzler, Director of the Smithsonian Caribbean Coral Reef Ecosystem Program, for his encouragement in pursuing the hydrological aspect of the mangrove ecosystem; Michael Carpenter, Smithsonian Institution (SI), for logistic support that made the fieldwork possible; Molly Ryan (SI) for her most useful and beautiful artwork; and George Venable (SI) for his computer-animated graphics that greatly aided our interpretation of the complex water movement in the mangrove swamps. We are grateful for financial support that was provided by the Exxon Corporation, the National Science Foundation Biocomplexity Grant to I. C. Feller (DEB-9981535), and the Smithsonian Institution. This is contribution number 852 of the Caribbean Coral Reef Ecosystems Program, Smithsonian Institution, and was supported in part by the Hunterdon Oceanographic Research Fund.

LITERATURE CITED

Alongi, D. M. 2002. Present State and Future of the World's Mangrove Forests. *Environmental Conservation*, 24:331–349.

Alongi, D. M., and A. D. McKinnon. 2005. The Cycling and Fate of Terrestrially-Derived Sediments and Nutrients in the Coastal Zone of the Great Barrier Reef Shelf. *Marine Pollution Bulletin*, 51:239–252.

Ball, M. C. 1988. Salinity Tolerance in the Mangroves *Aegiceras corniculatum* and *Avicennia maria*. I. Water Use in Relation to Growth, Carbon Partitioning, and Salt Balance. *Australian Journal of Plant Physiology*, 15:447–464.

Barbier, E. B. 2006. Natural Barriers to Natural Disasters: Replanting Mangroves After the Tsunami. *Frontiers in Ecology and the Environment*, 4(3):124–131.

Boulton, A. J., and M. A. Brock. 1999. *Australian Freshwater Ecology: Processes and Management*. Adelaide, Australia: Gleneagles Publishing.

Bryce, S., P. Larcombe, and P. V. Ridd. 2003. Hydrodynamics and Geomorphological Controls on Suspended Sediment Transport in Mangrove Creek Systems, a Case Study: Cocoa Creek, Townsville, Australia. *Estuarine, Coastal and Shelf Science*, 56:415–431.

Costanza, R., O. Perez-Maquco, M. L. Martinez, P. Sutton, S. L. Anderson, and K. Mulder. 2008. The Value of Coastal Wetlands for Hurricane Protection. *Royal Swedish Academy of Sciences*, 37(4):241–248.

Danielson, F., M. K. Sørenson, M. F. Olwig, V. Selvam, F. Parish, N. D. Burgess, T. Hiraishi, V. M. Karunagaran, M. S. Rasmussen, L. B. Hansen, A. Quarto, and N. Suryadiputra. 2005. The Asian Tsunami: A Protective Role for Coastal Vegetation. *Science*, 310:643.

Doyle, T. W. 2003. Effects of Hydrology on Red Mangrove Recruits. U. S. Geological Survey Report USGS 023-03. Lafayette, La.: National Wetlands Research Center.

Duke, N. C., J. O. Meynecke, S. Dittman, A. M. Ellison, K. Anger, U. Berger, C. Cannicci, K. Diele, K. C. Ewell, C. D. Field, N. Koedam, S. Y. Lee, C. Marchand, I. Nordhaus, and F. Dahdouh-Guebes. 2007. A World Without Mangroves? *Science*, 317:41–42.

Dunne, T., and L. B. Leopold. 1978. *Water in Environmental Planning*, pp. 135–138. San Francisco: W. H. Freeman and Company.

Feller, I. C., K. McKee, D. F. Whigham, and J. P. O'Neill. 2003. Nitrogen vs. Phosphorous Limitation across an Ecotonal Gradient in Mangrove Forest. *Biogeochemisty*, 62:145–175.

Feller, I. C., D. F. Whigham, J. P. O9Neil, and K. M. Mckee. 1999. Effect of Nutrient Enrichment Within-Stand Nutrient Cycling in Mangrove Ecosystems in Belize. *Ecology*, 80:2193–2205.

Forman, R. T. T., and M. Godron. 1986. *Landscape Ecology*. New York: John Wiley and Sons.

Furukawa, K., and E. Wolanski. 1996. Sedimentation in Mangrove Forests. *Mangroves and Salt Marshes*, 1:3–10.

Hutchings, P. A., and P. Saenger. 1987. *Ecology of Mangroves*. St. Lucia: University of Queensland Press.

Kjerfve, B., K. Rützler, and G. H. Kierspe. 1982. "Tides at Carrie Bow Cay, Belize." In *The Atlantic Barrier Reef Ecosystem at Carrie Bow Cay, Belize*, ed. K. Rützler and I. G. Macintyre. *Smithsonian Contributions to the Marine Sciences*, 12:47–51.

Knight, J. M., P. E. R. Dale, R. J. K. Dunn, G. J. Broadbent, and C. J. Lemckert. 2008. Patterns of Tidal Flooding within a Mangrove Forest: Coombabah, Southeast Queensland, Australia. *Estaurine, Coastal and Shelf Science*, 76:580–593.

Kobashi, D., and Y. Mazda. 2005. Tidal Flow in Riverine-type Mangroves. *Wetlands Ecology and Management*, 13:315–619.

Lindsley, R. K., and J. B. Franzini. 1979. *Water Resources Engineering (Open Channel)*. New York: McGraw Hill, pp. 251–256.

Lovelock, C. E. 2008. Soil Respiration and Belowground Carbon Allocation in Mangrove Forests. *Ecosystems*, 11:342–354.

Lugo, A. E., and S. C. Snedaker. 1974. The Ecology of Mangroves. *Annual Review of Ecology and Systematics*, 5:39–64.

Macintyre, I. G., and M. A. Toscano. 2004. The Pleistocene Limestone Foundation below Twin Cays, Belize, Central America. *Atoll Research Bulletin*, 511:1–16.

Macintyre, I. G., M. A. Toscano, I. C. Feller, and M. Faust. 2009. Decimating Mangrove Forests for Commercial Development in the Pelican Cays, Belize: Long-Term Ecological Loss for Short-Term Gain? *Smithsonian Contributions to the Marine Sciences*, No. 38:281–289.

Macintyre, I. G., M. A. Tocsano, R. G. Lightly, and G. B. Bond. 2004. Holocene History of the Mangrove Islands of Twin Cays, Belize, Central America. *Atoll Research Bulletin*, 510:1–16.

Mazda, Y., N. Knazawa, and T. Kurokawa. 1999. Dependence of Dispersion on Vegetation Density in a Tidal Creek-Mangrove Swamp System. *Mangrove and Salt Marshes*, 3(1):59–66.

Mazda, Y., D. Kobashi, and S. Okada. 2005. Tidal Scale Hydrodynamics Within Mangrove Swamps. *Wetlands Ecology and Management*, 13:647–655.

Mazda, Y., E. Wolanski, B. King, A Sase, O. Otsuka, and M. Magi. 1997. Drag Forces due to Vegetation in Mangrove Swamps. *Mangroves and Salt Marshes*, 1:193–199.

McKee, K. L., D. Cahoon, and I. C. Feller. 2007. Caribbean Mangroves Adjust to Rising Sea Level Through Biotic Controls on Soil Elevation Change. *Global Ecology and Biogeography*, 16:546–556.

Odum, W. E., and E. J. Heald. 1972. Trophic Analyses of an Estuarine Mangrove Community. *Bulletin of Marine Science*, 22:671–738.

———. 1975. "The Detritus-Based Food Web of an Estaurine Mangrove Community." In *Estaurine Research*, ed. L. E. Cronin, pp. 265–286. New York: Academic Press.

Rodriguez, W., and I. C. Feller. 2004. Mangrove Landscape Characterization and Change in Twin Cays, Belize Using Aerial Photography and IKONOS Satellite Data. *Atoll Research Bulletin*, 513:1–22.

Rützler, K., and I. C. Feller. 1988. Mangrove Swamp Communities. *Oceanus*, 30(4):16–24.

———. 1996. Caribbean Mangrove Swamps. *Scientific American*, 274(3):94–99.

Rützler, K., and J. D. Ferrais. 1982. "Terrestrial Environment and Climate, Carrie Bow Cay, Belize." In *The Atlantic Barrier Reef Ecosystem at Carrie Bow Cay, Belize*, ed. K. Rützler and I. G. Macintyre. *Smithsonian Contributions to the Marine Sciences*, 12:77–91.

Rützler, K., and I. G. Macintyre. 1982. "Introduction." In *The Atlantic Barrier Reef Ecosystem at Carrie Bow Cay, Belize*, ed. K. Rützler and I. G. Macintyre. *Smithsonian Contributions to the Marine Sciences*, 12:1–7.

Taylor, D. S., E. A. Reyier, W. P. Davis, and C. C. McIvor. 2007. Mangrove Removal in the Belize Cays: Effects on Mangrove-Associated Fish Assemblages in the Intertidal and Subtidal. *Bulletin of Marine Science*, 80(3):879–890.

Thornwaithe, C. W., and J. R. Mather. 1987. *Instructions and Tables for Computing Potential Evapo-transpiration and the Water Balance*, pp. 185–311. Centerton, N.J.: Laboratory of Climatology.

Tomlinson, P. B. 1986. *The Botany of Mangroves*. London: Cambridge University Press.

Toscano, M. A., and I. G. Macintyre. 2003. Corrected Western Atlantic Sea-Level Curve for the Last 11,000 Years Based on Calibrated ^{14}C Dates from *Acropora palmate* Framework and Intertidal Mangrove Peat. *Coral Reefs*, 22:257–270.

Twilley, R. R. 1988. "Coupling of Mangroves to the Productivity of Estuarine and Coastal Waters." In *Coastal Offshore Biosystem Interactions*, ed. B. O. Jansson, pp. 155–180. Berlin: Springer-Verlag.

———. 1995. "Properties of Mangrove Ecosystems in Relation to the Energy Signature of Coastal Environments." In *Maximum Power*, ed. G. A. S. Hall, pp. 43–62. Boulder: University Press of Colorado.

Urish, D. W., R. M. Wright, and O. Viator. 2003. *Topographic and Hydrographic Study in the Overwash Mangrove Islands of Twin Cays, Belize*. CCRE Report for 2002–2003. Washington, D.C.: Smithsonian Institution, National Museum of Natural History.

Watson, I., and A. D. Burnett. 1995. *Hydrology: An Environmental Approach*, pp. 460–465. Boca Raton, Fla.: CRC Press.

Wolanski, E., M. Jones, and J. S. Bunt. 1980. Hydrodynamics of a Tidal Creek-Mangrove Swamp System. *Australian Journal of Marine and Freshwater Research*, 31:431–450.

Wolanski, E., Y. Mazda, and P. Ridd. 1992. Mangrove Hydrodynamics. *Coastal and Estuarine Studies (Tropical Mangrove Ecosystems)*, 41:43–62.

Wolf, P. R., and C. D. Ghilani. 2006. *Elementary Surveying: An Introduction to Geomatics*, pp. 72–144. Upper Saddle River, N. J.: Pearson Prentice and Hall.

Wright, R. W., D. W. Urish and I. Runge. 1991. The Hydrology of a Caribbean Mangrove Island. In *Coastlines of the Caribbean, Coastal Zone '91 Conference-ASCE, Long Beach, CA July 1991*, ed. G. Cambers, pp. 171–184. New York: American Society of Civil Engineers.